Environmental Pollution 314 (2022) 120197

Contents lists available at ScienceDirect

Environmental Pollution

journal homepage: www.elsevier.com/locate/envpol

Urban edge trees: Urban form and meteorology drive elemental carbon deposition to canopies and soils☆

Alexandra G. Ponette-González [a,*], Dongmei Chen [b,1], Evan Elderbrock [c], Jenna E. Rindy [a,2], Tate E. Barrett [a,3], Brett W. Luce [a], Jun-Hak Lee [c], Yekang Ko [c], Kathleen C. Weathers [d]

[a] Department of Geography and the Environment, University of North Texas, 1155 Union Circle #305279, Denton, TX 76203, USA
[b] Department of Geography, 1251 University of Oregon, Eugene OR 97403-1251, USA
[c] Department of Landscape Architecture, 5249 University of Oregon, Eugene, OR 97403-5249, USA
[d] Cary Institute of Ecosystem Studies, Box AB, Millbrook, NY 12545, USA

ARTICLE INFO

Keywords:
Air quality
Edge effects
Elemental carbon
Particulate matter
LiDAR
Throughfall

ABSTRACT

Urban tree canopies are a significant sink for atmospheric elemental carbon (EC)—an air pollutant that is a powerful climate-forcing agent and threat to human health. Understanding what controls EC deposition to urban trees is therefore important for evaluating the potential role of vegetation in air pollution mitigation strategies. We estimated wet, dry, and throughfall EC deposition for oak trees at 53 sites in Denton, TX. Spatial data and airborne discrete-return LiDAR were used to compute predictors of EC deposition, including urban form characteristics, and meteorologic and topographic factors. Dry and throughfall EC deposition varied 14-fold across this urban ecosystem and exhibited significant variability from spring to fall. Generalized additive modeling and multiple linear regression analyses showed that urban form strongly influenced tree-scale variability in dry EC deposition: traffic count as well as road length and building height within 100–150 m of trees were positively related to leaf-scale dry deposition. Rainfall amount and extreme wind-driven rain from the direction of major pollution sources were significant drivers of throughfall EC. Our findings indicate that complex configurations of roads, buildings, and vegetation produce "urban edge trees" that contribute to heterogeneous EC deposition patterns across urban systems, with implications for greenspace planning.

1. Introduction

Cities are a major source and sink for carbonaceous particulate matter (PM; Bond et al., 2013; Barrett et al., 2019; Xu et al., 2021), which includes organic carbon and a refractory fraction distinguished by composition and method of determination. Atmospheric elemental carbon (EC) is the thermally stable fraction of PM that is determined using thermal or thermal-optical methods, whereas black carbon (BC) is the light-absorbing component determined using light absorption and optical methods (Petzold et al., 2013). Elemental carbon and BC are harmful air pollutants and, although atmospherically short-lived, play an important role in climate forcing (Masson-Delmotte et al., 2021). By-products of incomplete fossil fuel and biomass combustion, suspended EC and BC contribute to reduced visibility (Hand et al., 2020), air quality (e.g., Janssen et al., 2011), and health outcomes for urban populations (e.g., Alexeeff et al., 2018; Southerland et al., 2021). Moreover, these carbonaceous particles have strong warming potential: for example, during 100 yr after emission, 1 kg of BC produces, on average, as much warming as 680 kg of CO_2 (Bond and Sun, 2005).

Only two processes remove EC and BC from the atmosphere: wet and dry deposition. Although there are relatively few empirical estimates of urban wet and dry EC and BC deposition (Barrett et al., 2019), recent research indicates that tree leaves and canopies represent a significant sink for EC and BC in the urban landscape (Hara et al., 2014; Rindy et al., 2019; Byčenkienė et al., 2022). Rindy et al. (2019) estimated that urban trees have the potential to remove up to 30% of local vehicular EC

☆ This paper has been recommended for acceptance by Admir Créso Targino.

* Corresponding author.
E-mail address: alexandra.ponette@unt.edu (A.G. Ponette-González).
[1] Present address: Lane Council of Governments, 859 Willamette St #500, Eugene, OR 97401.
[2] Present address: Department of Biology, Boston University, 5 Cummington Mall, Boston, MA 02215.
[3] Present address: Barrett Environmental, 2209 St. Andrews, McKinney, TX 75072.

https://doi.org/10.1016/j.envpol.2022.120197
Received 16 April 2022; Received in revised form 13 September 2022; Accepted 13 September 2022
Available online 19 September 2022

emissions in a medium-sized city. Further, EC and BC delivered from canopies to the ground in throughfall, stemflow, and litterfall (Rindy et al., 2019; Van Stan et al., 2021) can become incorporated into soil through physical, chemical, and biological mechanisms (Czimczik and Masiello, 2007). Edmondson et al. (2015) found higher soil BC accumulation under tree canopies compared to areas without canopy cover, presumably due to higher inputs of BC from dry deposition washoff and leaf litterfall and subsequent mixing of BC into soils. Thus, vegetation in urban systems can contribute to both short- and long-term EC and BC sequestration.

High-resolution measurements of atmospheric BC in urban areas (e.g., Apte et al., 2017) nevertheless suggest that deposition of these particles to urban vegetation likely varies considerably across space and time. Mobile monitoring campaigns show that peak-to-median ratios of atmospheric BC vary 3-fold among census blocks (0.01 km^2; Chambliss et al. 2021), while data analysis from distributed networks of fixed sensors show 2-fold variation in BC concentrations in urban atmospheres on sub-daily and daily timescales (Caubel et al., 2019). In addition to spatially variable atmospheric concentrations, meteorology, topography, and urban form factors (i.e., the spatial organization and arrangement of people, buildings, infrastructure, and greenspace; Bereitschaft and Debbage, 2013) also influence atmospheric deposition (Weathers and Ponette-González, 2011; Decina et al., 2020). Seasonal variations in emissions and meteorological conditions as well as distance to road have been shown to affect EC and BC deposition rates to forests (Matsuda et al., 2012) and urban vegetation (Mori et al., 2018).

Given the potentially heterogeneous patterns of EC and BC inputs to urban canopies and soils, determining what controls intraurban variation in EC and BC deposition is important for developing targeted greenspace interventions aimed at mitigating air pollution within cities. Therefore, the specific objectives of this study were to: (1) quantify wet and dry EC deposition to, and throughfall EC deposition under, two urban oak tree species; and (2) model the spatiotemporal drivers of dry and throughfall EC deposition.

2. Materials and methods

2.1. Study area

We conducted this research in the City of Denton, Texas, a medium-sized city (pop. 139,734; U.S. Census Bureau, 2020) in the Dallas-Fort Worth metropolitan area, the fourth largest metropolitan area in the U.S. Climate in Denton is mild and temperate: mean annual temperature is 19 °C ± 1 (SD) and mean annual rainfall is 925 mm ± 270 (SD) (1991–2020, MESONET 2022). Precipitation is relatively evenly distributed throughout the year, with pulses of elevated rainfall in April–May and September–October. Prevailing winds are from the south during spring and summer, and from the north and south in fall and winter. Mean monthly wind speeds are highest in spring (20 km h^{-1} ± 1 SD) and winter (18 km h^{-1} ± 0.7 SD) and lower in summer (16 km h^{-1} ± 1 SD) and fall (16 km h^{-1} ± 1 SD).

Denton's geographic position downwind of Dallas-Fort Worth and Interstate 35, a major transportation corridor linking Denton to Dallas and Fort Worth (Fig. 1), leads to elevated PM concentrations in the area, especially when winds blow from the south (Luce et al., 2020). Atmospheric EC concentrations in $PM_{2.5}$ (<2.5 μm aerodynamic diameter) monitored by the Chemical Speciation Network in the City of Dallas (mean = 0.62 μg m^{-3} ± 0.07 SD, 2017–2021) are well above U.S. rural background levels (0.1–0.3 μg m^{-3}; Hand et al., 2013).

2.2. Elemental carbon deposition sampling

We measured EC in wet (rainfall), dry (particles), and throughfall (water that falls through and drips from canopy surfaces) deposition at sites distributed across the City of Denton between 29 March 2017 and 27 March 2018. Wet and throughfall deposition sites were selected using a stratified sampling design. The city was stratified by distance to major roads with truck traffic (0–100 m, >100 m) as diesel-powered vehicles represent the dominant source of EC emissions in U.S. urban areas (EPA, 2019). A 100-m cutoff was used because atmospheric BC concentrations show a >50% drop within 100 m of roads (Apte et al., 2017; Karner et al., 2010; Zhu et al., 2002). We selected sites in residential yards and urban greenspaces where samplers were unlikely to be disturbed or stolen.

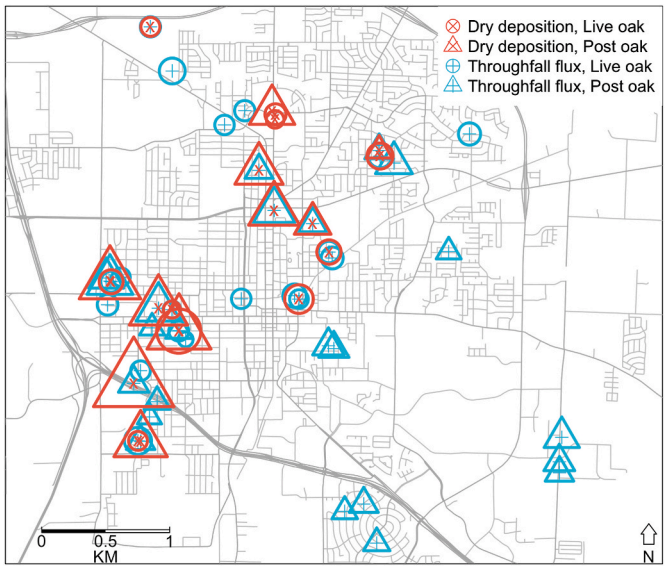

Fig. 1. Spatial patterns of elemental carbon (EC) deposition to urban tree canopies and soils in the City of Denton, Texas, sampled from March 2017 to March 2018. Symbol sizes are proportional to magnitude and show mean dry EC deposition (red; 0.07–0.97 mg m^{-2} d^{-1}) and mean throughfall EC deposition (blue; 0.03–0.43 mg m^{-2} d^{-1}) per tree for post oak (triangle) and live oak (circle) trees. Grey lines show roads in the City of Denton. The junction between I-35 E and I-35 W can be seen in the southwestern corner of the map. (For interpretation of the references to color in this figure legend, the reader is referred to the Web version of this article.)

Wet deposition was sampled at 16 sites without canopy cover, while throughfall EC was sampled under the canopies of 42 open-grown oak trees (i.e., without overlapping crowns from neighboring trees). Denton's urban tree canopy covers 30% of the city (State of the Denton Urban Forest, 2016), and post oak (*Quercus stellata* Wang.) and live oak (*Quercus virginiana* Mill.) rank 3rd and 14th, respectively, in terms of total citywide leaf area (i.e., one-sided leaf surface area, m^2; State of the Denton Urban Forest, 2016). Thus, post oak, a native deciduous tree, and live oak, a non-native evergreen tree, were selected for throughfall deposition sampling (n = 23 post oak, n = 19 live oak) given their abundance in the greater Dallas-Fort Worth area and southern U.S. cities.

Both tree species have similar mean height (15 m) and leaf area index (LAI, one-sided leaf surface area per ground surface area, m^2 m^{-2}), with a mean LAI of 2.4 and 3.4 for post oak and live oak, respectively. With regard to leaf characteristics, post oak leaves have two distinct sides: a shiny, dark green, and roughly textured upper surface with sparse trichomes and a light green, lower surface covered with abundant trichomes. Mature live oak leaves have a thick, shiny upper surface with few to no trichomes and a lower surface with densely packed trichomes. Post oak leaves are larger (mean surface area = 244 cm^2) and lobed with deeply indented margins, while live oak leaves are smaller (mean surface area = 133 cm^2) and have an oval, oblong, or elliptical shape with entire margins (Rindy et al., 2019).

Wet and throughfall collectors consisted of a 10-cm diameter borosilicate glass funnel set on a 500 ml amber glass bottle and placed within a PVC tube affixed to an iron rod established 1-m above ground. The

funnel rim sat above the edge of the PVC to prevent water from dripping into the funnel. One throughfall sampler was established midway between the bole and the canopy dripline on the south-facing side of each tree (i.e., the direction of prevailing winds and dominant EC emissions sources).

Wet and throughfall deposition were sampled on an event basis. A rainfall event was defined as producing a minimum of 2.5 mm of precipitation and separated from other rainfall periods by at least a 6-hr dry period (Lovett and Lindberg, 1984). Twenty-four hours prior to a forecasted rainfall event expected to produce a minimum of 2.5 mm, clean glass funnels and bottles were deployed to the sites (*Supporting Information*). Funnels and bottles were collected within 24 h after rainfall ceased, immediately transported to the laboratory, and refrigerated at 4 °C. One to two field blanks were included with every rainfall event. A forecast of insufficient rain or time to deploy the samplers prevented us from sampling all rainfall events. Over the year-long sampling period, 20 of 35 rainfall events (57%), constituting approximately 40% of total annual rainfall, were sampled for wet and throughfall deposition.

In a related study, we measured dry EC deposition to 20 trees ($n = 10$ post oak, $n = 10$ live oak; Rindy et al., 2019), 17 of which were also sampled for throughfall. Leaves were sampled from the south-facing side of trees monthly during the growing season (April–November for post oak, April–March for live oak). Three clusters of leaves were collected from the middle section of the canopy, placed in paper bags, and transported to the laboratory for analysis. Details on sampling methodology can be found in Rindy et al. (2019). In total, we collected 187 wet deposition, 359 throughfall, and 200 dry deposition samples.

2.3. Laboratory filtration and extraction

Sample filtration and extractions were performed within 24–48 h of sample collection. Wet and throughfall samples were filtered for EC following a slightly modified method employed by Torres et al. (2014). Prior to filtration, samples were sonicated for 15 min and then shaken by hand for 15 s to minimize particle adherence to the surface of the collection bottles. Samples were subsequently pre-filtered through a Buchner funnel with a fritted glass disk (pore size 40–60 μm) to remove large organic material (e.g., plant debris, soil). To increase EC recovery, 1.5 g of $NH_4H_2PO_4$ per 100 ml of water were added to each sample. Samples were sonicated and shaken again and then refrigerated for 24 h. The following day, samples were filtered through a 13-mm diameter pre-baked (600 °C for 12 h) quartz fiber filter and dried in a desiccator for 24 h. One method blank was prepared for each rainfall event.

Dry EC deposition was determined using a two-step foliar extraction technique (after Dzierżanowski et al., 2011). Briefly, leaves were immersed in 250 ml of double deionized water to remove 'rain-washable' EC particles. Samples were then processed following the same protocol as the throughfall samples: $NH_4H_2PO_4$ salt was added to the rinsewater, and samples were sonicated for 15 min and shaken by hand prior to refrigeration. In the second step, leaf samples were extracted with 150 ml of chloroform to remove particles deposited inside leaf waxes. Water and chloroform extracts were filtered using the same process as throughfall samples. Additional details on leaf extractions can be found in Rindy et al. (2019).

2.4. Elemental carbon analysis

Elemental carbon concentrations were determined using a thermal-optical method (NIOSH-5040) on a Sunset Laboratory Organic Carbon/Elemental Carbon (OC/EC) Aerosol Analyzer (Sunset Laboratories, Inc., Tigard, OR). For quality assurance, one instrument blank was analyzed each time the instrument was turned on, and two sucrose spike samples [5 μl (17.58 μg C) and 10 μl (35.16 μg C)] were analyzed to ensure calibration after every 10 samples. The minimum detection limit for the instrument was 0.21 μg of EC per cm^2 of filter.

2.5. Synthesis of deposition drivers

To assess spatiotemporal drivers of dry and throughfall EC deposition, we computed 128 variables describing urban form (i.e., transportation, vegetation, and building characteristics), meteorology, and topography using GIS and airborne discrete-return LiDAR (Table S1).

2.5.1. Transportation drivers

For transportation, we collected annual average daily traffic (AADT) from the Texas Department of Transportation, which is provided with point coordinates (i.e., vector point data). Road spatial data were obtained from City of Denton Open Data and annual on-road CO_2 emissions from the Database of Road Transportation Emissions (DARTE; Gately et al., 2019). Inverse-distance weighting was used to derive AADT at the sampling sites. The weight of each observation used for interpolation was calculated as the multiplicative inverse of distance between the interpolated site and the observed site divided by the total of the multiplicative inverses of distances from all available observations to the interpolated site. Road length and road count were calculated using the Sum Line Lengths tool combined with the Create Grid tool in QGIS (QGIS, 2021). Additional variables included distance to nearest road, major road, and bus stop, as well as the cumulative length (e.g., for roads) and count (e.g., for bus stops). We created grids of various cell sizes (e.g., 50, 100, 150, 300, 500 m) to cover the sampling sites and summarized these variables within each grid cell (ESRI, 2019). For analysis, we selected a grid cell size of 150 m as this maximized data variation and minimized distance to trees. Point data on CO_2 emissions at the sampling sites were extracted from the annual on-road CO_2 1-km emissions grid.

2.5.2. Meteorological drivers

We downloaded daily meteorological data on wind speed (mean, max), humidity (min, mean, max), and sea level air pressure (min, mean, max) from Weather Underground (Weather Underground, 2022). We selected eight weather stations within Denton city limits with complete temporal coverage from March 2017 to March 2018. Data on the direction of the fastest 2-min and fastest 5-s wind were obtained from the National Oceanic and Atmospheric Administration (NOAA) Global Historical Climatology Network-Daily (GHCND). These data were used to characterize extreme wind speeds (Klink, 2015). Data on wind direction (5-min resolution) were downloaded from the Automated Surface Observing System (ASOS). We used rainfall volumes measured in the field during wet deposition sampling, Weather Underground, and NOAA data for location-based rainfall measurements. The median of the same-date precipitation from all available stations was used to determine dry and rainfall days. Wind direction and rainfall datasets include data for two months prior to sampling to cover antecedent dry days (i.e., the number of dry days prior to the sampling date and after the last rainfall event at the nearest weather station; Lovett and Lindberg, 1984). All meteorological variables were computed separately for antecedent dry days and for rainfall events. We used inverse-distance weighting to compute wind speed (mean, max), humidity (min, mean, max), air pressure (min, mean, max), and rainfall at the sampling sites. Wind direction was aggregated as mean wind direction in azimuth degrees and wind direction mode in cardinal directions. In the modeling step, wind direction in azimuth degrees was converted to sine and cosine values of wind direction.

2.5.3. Vegetation and building characteristics

Variables describing vegetation and building characteristics were computed using 4-band imagery from the National Agriculture Imagery Program (NAIP) and LiDAR point-cloud data provided by the North Central Texas Council of Governments. NAIP data were collected on 20 September 2016 and have 1-m^2 pixel resolution. LiDAR data were collected from January–March 2015 with an average spacing of 0.5 m. To distinguish between vegetation and buildings, we used NAIP data to

calculate the Normalized Difference Vegetation Index (NDVI). The NDVI compares red (R) and near-infrared (NIR) reflectance with wavelength ranges of 604–664 nm and 683–920 nm, respectively (Biediger, 2021; Sohn and Dowman, 2007), and is calculated as follows:

$$NDVI = (NIR - R)/(NIR + R) \quad (1)$$

We used the LiDAR data to create a 1-m^2 pixel resolution digital elevation model (DEM) and digital surface model (DSM) for the study area. A digital height model (DHM) was then produced by subtracting the DEM from the DSM. The entire height range of DHM data was inspected and compared with NAIP imagery to identify upper and lower limits for building and tree height in the study area. Based on this assessment, trees were classified as pixels with NDVI $\geq$0.25 and height between 2 and 28 m, while buildings were classified as pixels clusters of greater than 25 m^2 with NDVI $<$0.25 and height between 2 and 90 m. An accuracy assessment of the land cover classification data was conducted by generating three hundred randomly selected points for each land cover type (i.e., building, tree, and non-building/tree). Each point was classified using NAIP air photo interpretation, and a confusion matrix was computed to compare land cover classification and air photo interpretation results, yielding an overall accuracy of 92% (*kappa = 0.89*; Table S2). The area, mean, and maximum height of vegetation and buildings within 50- and 100-m Euclidean buffers around each sampling site were calculated in ArcMap 10.7 (ESRI, 2019). These distances were selected as we expected changes in surface roughness near trees to influence microscale meteorological conditions, pollutant dispersion, and deposition.

Topographic variables (i.e., slope, elevation, and aspect) were calculated for each sampling site using a 10-m^2 DEM, generated from the LiDAR-derived 1-m^2 DEM (ESRI, 2019). Slope, elevation, and aspect were then used to derive further landform variables including topographic position index, relative aspect, terrain exposure to the horizontal component of the wind flux, horizontal angle of wind flux, and terrain exposure toward the sloped wind flux (Antonić and Legović, 1999; *Supporting Information*).

2.6. Data analysis and modeling

Daily wet, dry, and throughfall EC deposition were calculated per tree for comparison and expressed in mg m^{-2} d^{-1}. To calculate daily values, estimates of leaf-scale dry deposition were divided by the number of antecedent dry days (rain-washable) and number of days since leaf emergence (wax-deposited). Leaf-scale dry deposition represents the sum of the rain-washable and wax-deposited EC fractions (Rindy et al., 2019). Wet and throughfall deposition were divided by the number of days with rainfall.

We examined spatial variability in dry and throughfall EC deposition among sample trees using the coefficient of divergence (COD), a statistic widely used in air quality studies to assess variability in atmospheric concentrations among sampling sites (Bell et al., 2011; Xie et al., 2012). The COD for 15 trees sampled for dry and throughfall EC during April to October 2017 was calculated to evaluate if dry or throughfall deposition processes exhibited differences in spatial variability. The COD is normalized and ranges from 0 to 1. Values approaching 0 indicate high similarity and values approaching 1 indicate low similarity among sites. A threshold of 0.2 has been used to distinguish between homogeneous ($<$0.2) and heterogeneous ($\geq$0.2) spatial distributions (Wilson et al., 2005).

Seasonal differences in daily deposition were examined using one-way ANOVA followed by Tukey's Honestly Significant Difference (HSD) test. Samples were grouped into seasons: spring (March-April-May), summer (June-July-August), fall (September-October-November), and winter (December-January-February). Detailed calculations and equations are provided in the *Supporting Information*.

We performed an exploratory analysis of the data using generalized additive modeling (GAM; Chambers et al., 1990). GAM was employed as part of the variable selection process, specifically to understand the relative influence of drivers on EC deposition processes and potential nonlinear patterns in the data. Data transformations were performed on variables showing nonlinear relationships with EC deposition. Details regarding the GAM analysis are provided in the *Supporting Information*.

Multiple linear regression analysis was then employed to assess spatiotemporal drivers of dry and throughfall EC deposition. GAM-selected variables and their transformations were included in this analysis, and stepwise regression was implemented to further select the variables with the best fit and interpretability. We assessed model assumptions and collinearity using various diagnostic statistics and examined the significance of categorical variables using ANOVA (*Supporting Information*).

In the above modeling process, site index was included to account for repeated measurements of EC deposition at the same site. We also used simple linear regression to examine relationships between mean, median, minimum, maximum, and 95th percentile dry EC and throughfall EC deposition and aggregated predictor variables (i.e., mean of predictor variables, such as road length within 150 m of trees) to provide further insights on the influence of location-specific variables such as urban form and traffic volume on dry and throughfall EC deposition. All analyses were performed in R. Significance was set to $p < 0.05$.

3. Results

3.1. Spatial and temporal patterns of EC deposition

Dry EC deposition to urban trees ranged 14-fold from 0.07 to 0.97 mg m^{-2} d^{-1}, with a mean of 0.38 mg m^{-2} d^{-1}, while throughfall EC deposition ranged 0.03–0.43 mg m^{-2} d^{-1}, with a mean of 0.18 mg m^{-2} d^{-1} (Fig. 1). Five trees sampled for dry, and five trees sampled for throughfall deposition had values $>$ 50% higher than the overall mean. Mean rates of dry and throughfall deposition were 4-fold and 2-fold higher, respectively, compared to wet deposition (mean = 0.1 mg m^{-2} d^{-1}), which also had a smaller range of values (0.04–0.33 mg m^{-2} d^{-1}). For trees with both dry and throughfall EC deposition measurements (n = 17 trees), throughfall EC comprised 13–73% (mean = 40%) of wet plus dry EC deposition.

Both dry and throughfall deposition had coefficient of divergence (COD) values $\geq$ 0.2, indicating heterogeneous spatial distributions (Table S3, Table S4). Dry deposition of EC was, however, more spatially heterogeneous than throughfall EC, as indicated by the mean COD for trees sampled (dry deposition = 0.62; throughfall deposition = 0.56). We found no difference in the mean COD value between species for dry or throughfall deposition (i.e., species were similarly spatially variable). We also examined COD values by location within the city. Trees sampled for dry deposition in the southwestern part of the city had significantly higher COD values compared to trees in the northeast ($p < 0.05$) whereas throughfall COD values did not differ by location.

Elemental carbon in wet, dry, and throughfall deposition also exhibited seasonal variability. Both wet and throughfall deposition were highest in spring and lowest in the fall and winter ($p < 0.05$). Throughfall deposition and dry deposition showed an inverse seasonal relationship, a pattern that was consistent for both tree species (Fig. 2).

3.2. Spatiotemporal drivers of EC deposition

Multiple linear regression analysis showed that the most important drivers of dry EC deposition were month (i.e., all months compared to April in model), number of antecedent dry days, and maximum daily relative humidity (Table 1, Table S5). Although the number of antecedent dry days was negatively related to daily dry deposition in the model, cumulative dry deposition had a significant but weak positive correlation with antecedent dry days (Fig. S1). Maximum daily relative humidity was also a significant negative, albeit weak predictor of dry EC

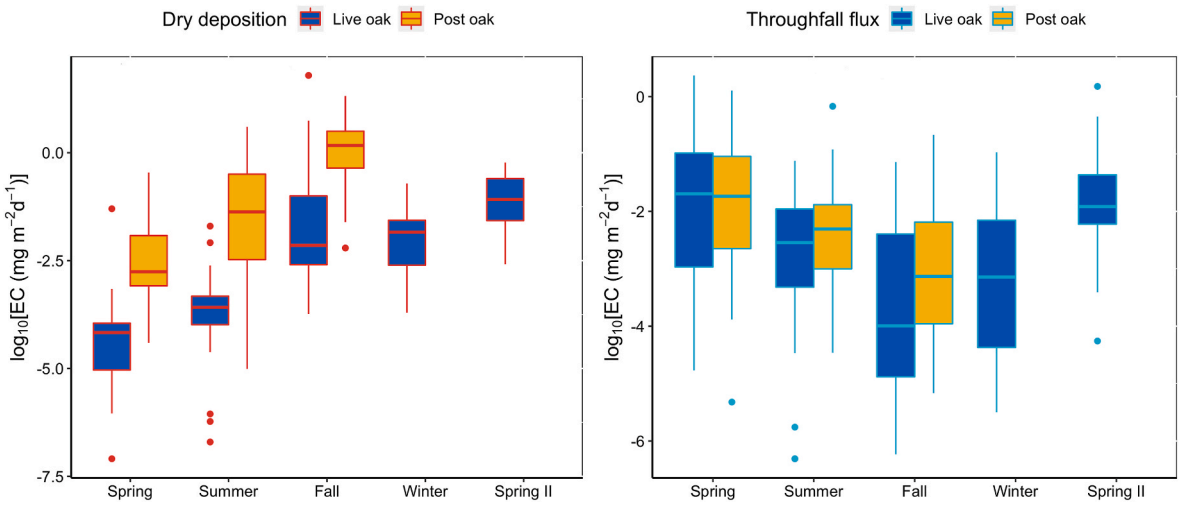

Fig. 2. Seasonal patterns of elemental carbon (EC) deposition to urban tree canopies and soils in the City of Denton, Texas, sampled from March 2017 to March 2018. Spring II denotes samples collected after 2018 leaf flush. Boxplots show dry deposition (red outline, left) and throughfall (blue outline, right) by season and by species. Whiskers show the highest and lowest values, excluding outliers, which are shown as dots. (For interpretation of the references to colour in this figure legend, the reader is referred to the Web version of this article.)

Table 1
Multiple linear regression results for dry and throughfall deposition of elemental carbon (EC) (mg m^{-2} d^{-1}).

Dry Deposition *(n = 200; adjusted R^2 = 0.79)*			Throughfall Flux *(n = 359; adjusted R^2 = 0.44)*		
Variable	Estimated Coefficient	t-statistic	Variable	Estimated Coefficient	t-statistic
Intercept	−3.7	−13 ***	Intercept	0.596	12 ***
Index[a]	n/a	13 ***	Index[a]	n/a	2.1 ***
Month[b]	n/a	48 ***	Wind direction[b]	n/a	7.6 ***
Antecedent dry days	-4.9×10^{-2}	−2.6 **	Antecedent dry days	-3.3×10^{-3}	−4.4 ***
Max relative humidity	-5.9×10^{-2}	−3.5 ***	Fastest 2-min wind (west-east)	-7.1×10^{-2}	−6.0 ***
			Cumulative rainfall	-5.5×10^{-3}	−3.2 **
			Cumulative rainfall (squared)	1.0×10^{-4}	3.6 ***
			Wet EC deposition	4.0×10^{-2}	5.3 ***

*$p < 0.05$, **$p < 0.01$, ***$p < 0.001$.
[a] Compared each location to Index1; F-statistic from ANOVA analysis included rather than the t-statistic from regression model. See Tables S5 and S6 for complete model summary.
[b] F-statistic from ANOVA analysis included rather than the t-statistic from regression model. See Tables S5 and S6 for complete model summary.

deposition (Table 1).

Several meteorological variables, including wind direction (i.e., northwesterly, southeasterly, and southwesterly winds compared to northeasterly wind in model) and wind speed, the number of antecedent dry days, cumulative precipitation, and wet EC deposition were significant predictors of throughfall EC (Table 1, Table S6). During rainfall events, extreme wind speeds originating from the west produced higher throughfall EC than similarly fast winds from the east (Fig. 3a). The mode, or most common, wind direction during dry days prior to a rainfall event was also influential in the model, with southeasterly and southwesterly winds showing the strongest positive associations with throughfall EC. We found a similar relationship between antecedent dry days and throughfall EC as with dry EC deposition: daily deposition was negatively related while cumulative deposition was positively related to the number of antecedent dry days (Fig. S1). Rainfall amount (Fig. 3b) and wet EC deposition both showed positive relationships with throughfall EC.

Simple linear regressions revealed significant positive relationships between dry EC deposition and aggregated values for urban form variables. Dry EC deposition was most strongly related to total road length within 150 m of trees, with R^2 values of 0.71 and 0.6 for mean and 95th percentile dry deposition, respectively (Fig. 4). Dry EC deposition also increased with daily traffic count, although the strength of this relationship was less strong than for total road length. Mean building height within 100 m of trees exhibited a positive relationship with mean and 95th percentile dry deposition. There were no significant relationships between total road length, traffic count, building height and throughfall EC deposition.

4. Discussion

4.1. Local-scale effects of urban form on dry deposition of elemental carbon

Urban trees are nested within spatially heterogeneous ecosystems composed of infrastructure, buildings, and greenspace. The presence, density, height, and spatial arrangement of these elements can vary substantially over short horizontal and vertical distances (Cadenasso et al., 2007), resulting in complex three-dimensional urban surfaces. Although interactions between this urban fabric and atmospheric pollutants may contribute to a "distinct urban biogeochemistry" (*sensu* Kaye et al., 2006), fine-scale drivers of deposition within cities remain elusive.

We were not surprised to find that dry deposition increased with road length (a measure of road proximity) and traffic count. Ambient BC concentrations are higher in areas associated with truck traffic, higher traffic volumes, and near (within a few hundred meters of) roadways (Karner et al., 2010; Clougherty et al., 2013; Apte et al., 2017; Caubel et al., 2019; Henneman et al., 2021). Moreover, edge effects—the filtering of atmospheric pollutants by vegetation at edges—are well

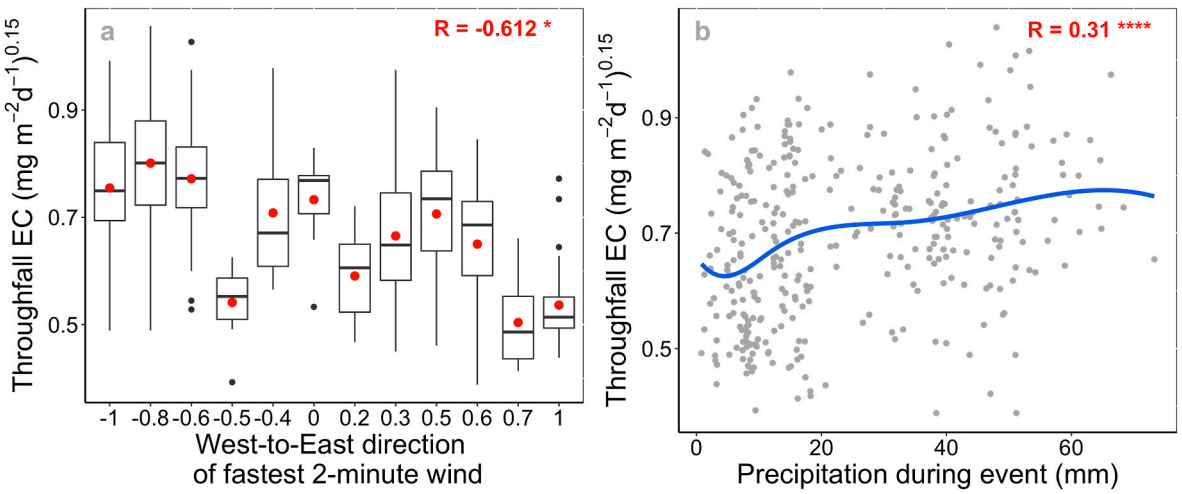

Fig. 3. Bivariate relationships between variables from the multiple linear regression analysis and throughfall elemental carbon (EC) deposition in the City of Denton, Texas, sampled from March 2017–March 2018. Variables include (a) the fastest 2-min wind (a proxy for extreme wind speeds) along a west-east direction (red dots indicate the mean of throughfall EC) and (b) rainfall amount during rainfall events. A five-degree spline shows the nonlinear relationship between rainfall amount and throughfall EC. The Pearson correlation R and level of significance (*$p < 0.05$, ****$p < 0.0001$) are labeled for reference. Whiskers show the highest and lowest values, excluding outliers, which are shown as dots. (For interpretation of the references to colour in this figure legend, the reader is referred to the Web version of this article.)

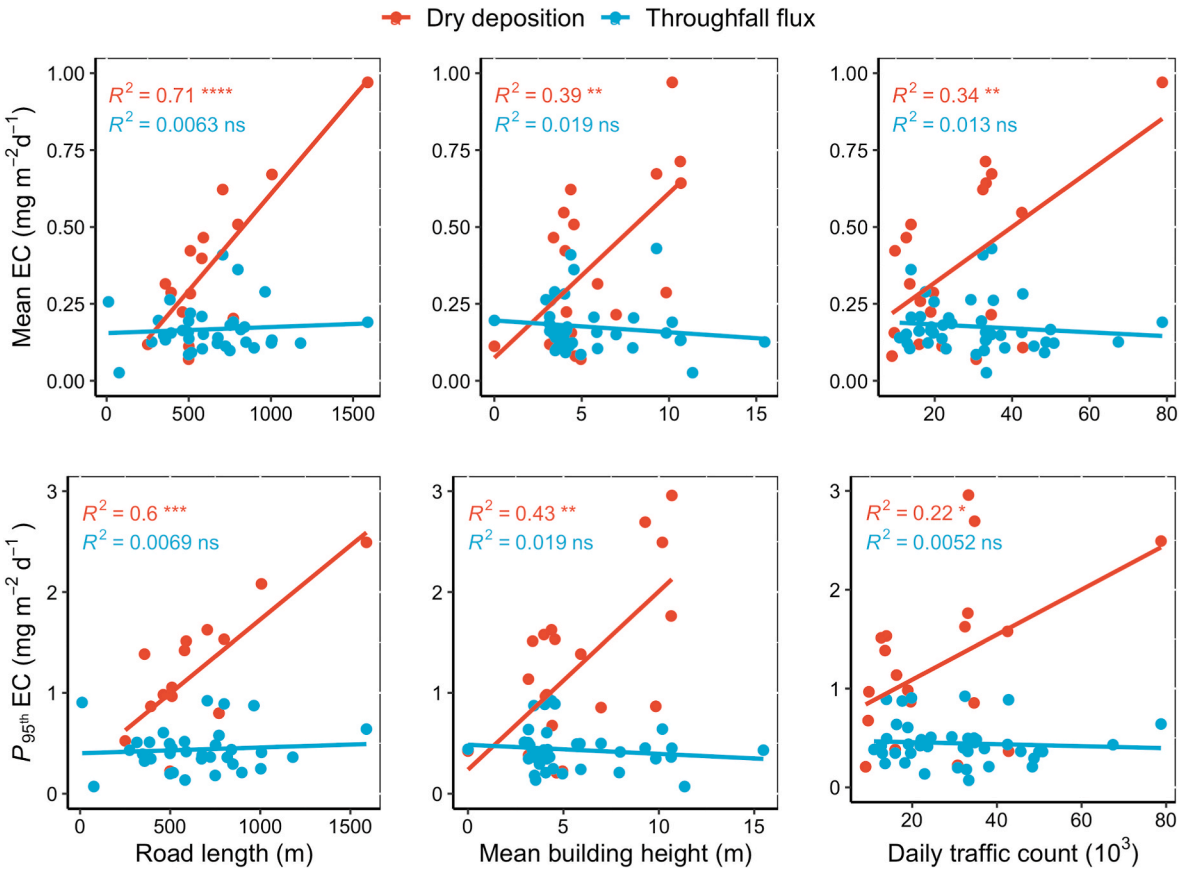

Fig. 4. Bivariate relationships between dry elemental carbon (EC) deposition (red dots) and throughfall EC deposition (blue dots) and urban form variables. Data are aggregated by total road length within 150 m, mean building height within 100 m , and daily traffic count (10^3), with functions of mean and 95th percentile. The R-squared and level of significance (*$p < 0.05$, **$p < 0.01$, ***$p < 0.001$, ****$p < 0.0001$) are labeled for reference. (For interpretation of the references to colour in this figure legend, the reader is referred to the Web version of this article.)

documented (e.g., Weathers et al., 2001; Ewing et al., 2009). For example, particulate deposition to tree leaves has been shown to differ between roadside and background environments by as much as 16-fold (Maher et al., 2008), often decreasing markedly within 75–150 m of roads (Kardel et al., 2012). Thus, that we detected near-road effects on dry EC deposition is consistent with steep urban roadway gradients in

both observed atmospheric BC concentrations *and* PM deposition.

Our data suggest, however, that road edge effects on EC deposition vary in magnitude due to differences in concentrations among road types (Apte et al., 2017). In our analysis, trees proximate to roads with high traffic volumes, such as Interstate-35, received dry EC inputs that were ~4-fold higher than trees near less busy roads. In Belgium, leaf PM accumulation increased exponentially with traffic intensity; although EC was not measured, the highest accumulation values were measured near highways and intersections (Kardel et al., 2012). Taken together, our data confirm that dry deposition of particulates (including EC) to leaf surfaces increases as a function of the strength of and proximity to emissions sources in urban areas (Maher et al., 2008; Kardel et al., 2012; Hofman et al., 2014; Rea-Downing et al., 2020).

Findings also revealed the role of building height on dry EC deposition to trees. In this urban ecosystem, where mostly low- and some mid-rise buildings are configured in an open arrangement, taller structures could be interpreted as indicative of more developed land cover (i.e., urban imperviousness), and hence increased travel-related emissions. Alternatively, where streets are flanked by buildings on both sides (i.e., street canyons; Vardoulakis et al., 2003), higher EC deposition to trees could be due to a classic canyon effect. It is well established that traffic emissions coupled with reduced wind dispersion of pollutants lead to elevated PM and BC air concentrations and deposition in street canyons (Boogaard et al., 2011; Pugh et al., 2012; Hofman et al., 2014; Abhijith et al., 2017; Liu et al., 2020), an effect that increases as canyons become deeper (i.e., as building height relative to street width increases; Pugh et al., 2012; Hofman et al., 2014). Tree-to-tree differences in dry EC deposition were also most pronounced in the southwestern part of the city where buildings are tallest and urban imperviousness is highest. This suggests that complex configurations of roads, buildings, and vegetation—and the edges they create and sustain (e.g., Amato et al., 2019)—contribute to spatially heterogeneous patterns of dry EC deposition in urban areas.

Superimposed on this intraurban variation in dry EC deposition to trees, we observed temporal changes in deposition inputs related to regional pollution patterns. In Dallas, airborne EC concentrations are lowest in late spring and early summer and increase steadily from late summer through fall, peaking in December. In Denton, dry EC deposition to urban trees follows a similar pattern. In fact, monthly atmospheric EC concentrations measured in Dallas during the time of sampling were positively related to our estimates of monthly dry EC deposition ($R^2 = 0.52, p < 0.01$; Fig. S2). This relationship indicates that regional EC emissions from the greater Dallas-Fort Worth metropolitan area drive temporal patterns in dry deposition but do not override the localized effects of urban form on dry deposition.

4.2. Mobilization of EC particles in throughfall by extreme wind and rain

Until recently, the composition and amount of PM in throughfall and stemflow have received relatively little attention (Lequy et al., 2014; Levia et al., 2013; Cayuela et al., 2019; Ponette-González et al., 2020; Xu et al., 2020; Van Stan et al., 2021), with only a few studies isolating the carbonaceous fraction (EC or BC). Here, we found that most EC deposited to urban trees accumulates in the canopy, with just 40% delivered to the ground in throughfall. The proportion of EC in throughfall was highest in late spring and lower in fall and winter, consistent with the speculation that dry EC deposition increases over time due, in part, to increasing leaf wettability (Rindy et al., 2019). Aside from leaf surface retention, EC can be retained on branch and stem bark surfaces (Ponette-González 2021) and/or incorporated into microbial biomass (Espenshade et al., 2019). In addition, some amount of EC is delivered to the ground via stemflow, while some EC can be lost from trees by pruning or other landscape activities. Accounting for these fluxes in future studies will improve estimates of canopy EC retention.

Our estimate of EC mobilization with throughfall is nonetheless well within the range of values reported for leaf-washing and rainfall simulation experiments that show that water can mobilize anywhere from 30 to 70% of particulates <100 μm from plant surfaces depending on plant species and functional type (Przybysz et al., 2014; Xu et al., 2017; Zhang et al., 2019). However, compared to coarse ($PM_{2.5}$-PM_{10}) and large (PM_{10}-PM_{100}) particles, fine particles (<2.5 μm diameter) are less efficiently removed by rainfall and wind (Levia et al., 2013; Przybysz et al., 2014; Cayuela et al., 2019; Popek et al., 2019) because of their high surface area-to-volume ratio and low resuspension rates (Wang et al., 2018; Xie et al., 2018). As urban EC is predominantly in the $PM_{2.5}$ fraction, our findings may be more comparable with those of Chen et al. (2017) who determined that, for broadleaf tree species (such as ours), simulated rainfall removed 47% of accumulated fine PM.

For biologically inactive particles such as EC, throughfall deposition results from the transport of wet- and dry-deposited particles to the ground. Thus, throughfall deposition is influenced by the factors that control particulate transport through the canopy (Van Stan et al., 2021) as well as wet and dry deposition (Weathers et al., 2006; Ponette-González et al., 2016). A few previous studies demonstrate positive relationships between the amount of PM deposited to and removed from tree leaves with simulated rain (Chen et al., 2017; Xu et al., 2017). We did not find a similar correlation between dry and throughfall EC deposition, likely due to differences in sampling strategy. However, wet EC deposition as well as winds from the direction of major pollution sources antecedent to rainfall events, which we have shown influence dry deposition, were important variables in the throughfall model.

Despite the potential for high canopy retention of EC, our model elucidates the meteorological conditions under which particles are mobilized and transported through tree canopies in throughfall. We know of only one study aside from ours to investigate PM wash-off dynamics from urban trees under natural conditions using the throughfall method. Consistent with our findings, Cai et al. (2019) found that for all size fractions the amount of PM in throughfall increased with rainfall amount. Our data further indicate that extreme winds lead to high rates of throughfall EC deposition when rainfall is driven from west to east. Wind-driven rain has been associated with increased stemflow production (Van Stan et al., 2011) and splash-saltation trajectories in soil erosion studies (Erpul et al., 2004). It is therefore plausible that wind-driven rain increases throughfall volume, detachment of EC from the canopy, or both, ultimately leading to greater EC deposition inputs to the surface. In our study area, the prevailing direction of storm tracks during the spring season is from southwest to northeast. Thus, wind-driven rain effects on throughfall amount and EC mobilization may also partly explain the spring spike we observed in throughfall deposition.

4.3. Implications for greenspace planning

Our findings have important implications for greenspace planning. First, roads and buildings represent structural discontinuities or “edges” (*sensu* Weathers et al., 2001, 2006) in urban ecosystems that expose vegetation to elevated pollution levels. Such discontinuities are common features in cities and result in the creation of “urban edge trees”, trees that receive higher levels of EC deposition than trees distant from edges. Where atmospheric deposition (i.e., removal) is identified as a possible mechanism for air pollution mitigation in greenspace interventions (Diener and Mudu, 2021), our findings underscore the need to further identify and model the combination of locations and configurations of urban morphology that are likely to have the greatest impact on deposition to canopies and linked fluxes to soils. Second, although infrequently measured, throughfall and stemflow represent important potential pathways for the delivery of particulates to soils following deposition. Elemental carbon deposited to the ground with water is less likely to be resuspended to the atmosphere and may be readily available for transport in water: downward into the soil or, if deposited to pavement, laterally via runoff into streams (Decina et al., 2018). Thus, the biogeochemical pathways of particulates after deposition are also

critical to consider when planning for air quality mitigation and/or long-term EC sequestration.

5. Conclusions

We present some of the first estimates of intraurban variation in EC deposition to urban tree canopies and soils. Our findings show that EC deposition exhibits high intraurban variability due to complex spatio-temporal drivers. Specifically, local-scale urban form factors coupled with regional-scale pollution and meteorology contribute to a 14-fold difference in EC deposition to canopies and soils across this urban ecosystem. Consistent with fine-scale studies of airborne BC concentrations, we detected strong near-road and street canyon "edge effects" on dry EC deposition that resulted in elevated levels of EC deposition to urban trees. While we estimate that 60% of this carbon is retained in tree canopies, results indicate that high rainfall coupled with extreme westerly winds mobilize and transport EC to the ground in throughfall.

Taken together, these findings could inform greenspace interventions focused on urban air quality, such as tree planting and conservation. Knowledge of the urban form factors that influence spatial patterns of EC deposition is crucial to predict where on the landscape tree canopies are likely to have the greatest impact on EC deposition at street-to-city scales. Further, our study suggests that the role of meteorology in driving EC transport in urban systems should be considered in tree-based air quality greenspace interventions. Integrating empirical and modeling approaches to predict and prioritize locations for tree planting and/or conservation represents a crucial next step in urban forest planning for air pollution mitigation.

Credit author statement

Conceptualization: AGPG, KCW; **Data curation**: DC, EE; **Formal analysis**: AGPG, DC, EE, JER; Funding **acquisition**: AGPG; **Investigation**: AGPG, JER, BWL, TEB; **Methodology**: DC, EE, TEB, JL, YK, KCW; **Project administration**: AGPG, YK; **Supervision**: AGPG, KCW; **Visualization**: DC; **Writing** – original draft: AGPG; **Writing** – review and editing: DC, EE, JER, TEB, BWL, JL, YK, KCW.

Declaration of competing interest

The authors declare that they have no known competing financial interests or personal relationships that could have appeared to influence the work reported in this paper.

Data availability

The data underlying this study will be available on the Knowledge Network for Biodiversity repository.

Acknowledgments

We are grateful to City of Denton residents, City of Denton Parks and Recreation, UNT Facilities, Texas Woman's University, Eco-W.E.R.C.S., and Denton Public Library North Branch for allowing us to conduct sampling in Denton's urban yards and greenspaces. We thank Cassidy Winter, Bethel Steele, and Eric Graham for field and lab assistance, the Editor and two anonymous reviewers for their constructive feedback on the manuscript. LiDAR data were provided by the North Central Texas Council of Governments. Support for this research was provided by the National Science Foundation (CAREER #1552410).

Appendix A. Supplementary data

Supplementary data to this article can be found online at https://doi.org/10.1016/j.envpol.2022.120197.

References

Abhijith, K.V., Kumar, P., Gallagher, J., McNabola, A., Baldauf, R., Pilla, F., Broderick, B., Di Sabatino, S., Pulvirenti, B., 2017. Air pollution abatement performances of green infrastructure in open road and built-up street canyon environments–A review. Atmos. Environ. 162, 71–86.

Alexeeff, S.E., Roy, A., Shan, J., Liu, X., Messier, K., Apte, J.S., Portier, C., Sidney, S., Van Den Eeden, S.K., 2018. High-resolution mapping of traffic related air pollution with google street view cars and incidence of cardiovascular events within neighborhoods in oakland, CA. Environ. Health 17 (1), 1–13.

Amato, F., Pérez, N., López, M., Ripoll, A., Alastuey, A., Pandolfi, M., Karanasiou, A., Salmatonidis, A., Padoan, E., Frasca, D., 2019. Vertical and horizontal fall-off of black carbon and NO2 within urban blocks. Sci. Total Environ. 686, 236–245.

Antonić, O., Legović, T., 1999. Estimating the direction of an unknown air pollution source using a digital elevation model and a sample of deposition. Ecol. Model. 124 (1), 85–95.

Apte, J.S., Messier, K.P., Gani, S., Brauer, M., Kirchstetter, T.W., Lunden, M.M., Marshall, J.D., Portier, C.J., Vermeulen, R.C.H., Hamburg, S.P., 2017. High-resolution air pollution mapping with google street view cars: exploiting big data. Environ. Sci. Technol. 51 (12), 6999–7008.

Barrett, T.E., Ponette-González, A.G., Rindy, J.E., Weathers, K.C., 2019. Wet deposition of black carbon: a synthesis. Atmos. Environ. 213, 558–567.

Bell, M.L., Ebisu, K., Peng, R.D., 2011. Community-level spatial heterogeneity of chemical constituent levels of fine particulates and implications for epidemiological research. J. Expo. Sci. Environ. Epidemiol. 21 (4), 372–384.

Bereitschaft, B., Debbage, K., 2013. Urban form, air pollution, and CO2 emissions in large US metropolitan areas. Prof. Geogr. 65 (4), 612–635.

Biediger, J., 2021. 2016 Texas Image Dates. NAIP Image Dates. https://naip-image-dates-usdaonline.hub.arcgis.com/datasets/b113fb8819bf4721a555296db29be18c_0/about.

Bond, T.C., Sun, H., 2005. Can reducing black carbon emissions counteract global warming? Environ. Sci. Technol. 39 (16), 5921–5926.

Bond, T.C., Doherty, S.J., Fahey, D.W., Forster, P.M., Berntsen, T., DeAngelo, B.J., Flanner, M.G., Ghan, S., Kärcher, B., Koch, D., 2013. Bounding the role of black carbon in the climate system: a scientific assessment. J. Geophys. Res. Atmos. 118 (11), 5380–5552.

Boogaard, H., Kos, G.P.A., Weijers, E.P., Janssen, N.A.H., Fischer, P.H., van der Zee, S.C., de Hartog, J.J., Hoek, G., 2011. Contrast in air pollution components between major streets and background locations: particulate matter mass, black carbon, elemental composition, nitrogen oxide and ultrafine particle number. Atmos. Environ. 45 (3), 650–658.

Byčenkienė, S., Pashneva, D., Uogintė, I., Pauraitė, J., Minderytė, A., Davulienė, L., Plauškaitė, K., Skapas, M., Dudoitis, V., Touqeer, G., 2022. Evaluation of the anthropogenic black carbon emissions and deposition on Norway spruce and silver birch foliage in the baltic region. Environ. Res. 207, 112218.

Cadenasso, M.L., Pickett, S.T.A., Schwarz, K., 2007. Spatial heterogeneity in urban ecosystems: reconceptualizing land cover and a framework for classification. Front. Ecol. Environ. 5 (2), 80–88.

Cai, M., Xin, Z., Yu, X., 2019. Particulate matter transported from urban greening plants during precipitation events in beijing, China. Environ. Pollut. 252, 1648–1658.

Caubel, J.J., Cados, T.E., Preble, C.V., Kirchstetter, T.W., 2019. A distributed network of 100 black carbon sensors for 100 Days of air quality monitoring in west oakland, California. Environ. Sci. Technol. 53 (13), 7564–7573.

Cayuela, C., Levia, D.F., Latron, J., Llorens, P., 2019. Particulate matter fluxes in a mediterranean mountain forest: interspecific differences between throughfall and stemflow in oak and pine stands. J. Geophys. Res. Atmos. 124 (9), 5106–5116.

Chambers, J., Hastie, T., Pregibon, D., 1990. Statistical models in S. In: Compstat. Springer, pp. 317–321.

Chambliss, S.E., Pinon, C.P.R., Messier, K.P., LaFranchi, B., Upperman, C.R., Lunden, M. M., Robinson, A.L., Marshall, J.D., Apte, J.S., 2021. Local-and regional-scale racial and ethnic disparities in air pollution determined by long-term mobile monitoring. Proc. Natl. Acad. Sci. USA 118 (37).

Chen, L., Liu, C., Zhang, L., Zou, R., Zhang, Z., 2017. Variation in tree species ability to capture and retain airborne fine particulate matter (PM2. 5). Sci. Rep. 7 (1), 1–11.

Clougherty, J.E., Kheirbek, I., Eisl, H.M., Ross, Z., Pezeshki, G., Gorczynski, J.E., Johnson, S., Markowitz, S., Kass, D., Matte, T., 2013. Intra-urban spatial variability in wintertime street-level concentrations of multiple combustion-related air pollutants: the New York city community air survey (NYCCAS). J. Expo. Sci. Environ. Epidemiol. 23 (3), 232–240.

Czimczik, C.I., Masiello, C.A., 2007. Controls on black carbon storage in soils. Global Biogeochem. Cycles 21 (3).

Decina, S.M., Templer, P.H., Hutyra, L.R., 2018. Atmospheric inputs of nitrogen, carbon, and phosphorus across an urban area: unaccounted fluxes and canopy influences. Earth's Future 6 (2), 134–148.

Decina, S.M., Ponette-González, A.G., Rindy, J.E., 2020. Urban tree canopy effects on water. Quality via inputs to the urban ground surface. In: Forest-water Interactions. Springer, pp. 433–457.

Diener, A., Mudu, P., 2021. How can vegetation protect us from air pollution? A critical review on. Green spaces' mitigation abilities for air-borne particles from a public health perspective-with implications for urban planning. Sci. Total Environ. 796, 148605.

Dzierżanowski, K., Popek, R., Gawrońska, H., Sæbø, A., Gawroński, S.W., 2011. Deposition of. Particulate matter of different size fractions on leaf surfaces and in waxes of urban forest species. Int. J. Phytoremediation 13 (10), 1037–1046.

Edmondson, J.L., Stott, I., Potter, J., Lopez-Capel, E., Manning, D.A.C., Gaston, K.J., Leake, J.R., 2015. Black carbon contribution to organic carbon stocks in urban soil. Environ. Sci. Technol. 49 (14), 8339–8346.
EPA, 2019. U. S. Integrated Science Assessment (ISA) for Particulate Matter. Agency USEP, Washington, DC, 2009.
Erpul, G., Gabriels, D., Norton, L.D., 2004. Sand detachment by wind-driven raindrops. Earth Surf. Process. Landforms J. Br. Geomorphol. Res. Gr. 30 (2), 241–250.
Espenshade, J., Thijs, S., Gawronski, S., Bové, H., Weyens, N., Vangronsveld, J., 2019. Influence of urbanization on epiphytic bacterial communities of the platanus× hispanica tree leaves in a biennial study. Front. Microbiol. 10, 675.
ESRI, 2019. ArcMap 10.7; Environmental Systems Research Institute. Redlands, CA, USA.
Ewing, H.A., Weathers, K.C., Templer, P.H., Dawson, T.E., Firestone, M.K., Elliott, A.M., Boukili, V.K.S., 2009. Fog water and ecosystem function: heterogeneity in a California redwood forest. Ecosystems 12 (3), 417–433.
Gately, C., Hutyra, L.R., Wing, I.S., 2019. DARTE Annual On-Road CO2 Emissions on a 1-km Grid, Conterminous USA, vol. 2. ORNL DAAC, Oak Ridge, Tennessee, USA. https://doi.org/10.3334/ORNLDAAC/1735, 1980-2017.
Hand, J.L., Schichtel, B.A., Malm, W.C., Frank, N.H., 2013. Spatial and temporal trends in PM2. 5. Organic and elemental carbon across the United States. Adv. Meteorol. 2013, 367674.
Hand, J.L., Prenni, A.J., Copeland, S., Schichtel, B.A., Malm, W.C., 2020. Thirty years of the clean air act amendments: impacts on haze in remote regions of the United States (1990– 2018). Atmos. Environ. 243, 117865.
Hara, H., Kashiwakura, T., Kitayama, K., Bellingrath-Kimura, S.D., Yoshida, T., Takayanagi, M., Murao, N., Okouchi, H, Ogata, H., 2014. Foliar rinse study of atmospheric black carbon deposition to leaves of konara oak (*Quercus serrata*) stands. Atmos. Environ. 97, 511–518.
Henneman, L.R.F., Shen, H., Hogrefe, C., Russell, A.G., Zigler, C.M., 2021. Four decades of United States mobile source pollutants: spatial–temporal trends assessed by ground-based monitors, air quality models, and satellites. Environ. Sci. Technol. 55 (2), 882–892.
Hofman, J., Lefebvre, W., Janssen, S., Nackaerts, R., Nuyts, S., Mattheyses, L., Samson, R., 2014. Increasing the spatial resolution of air quality assessments in urban areas: a comparison of biomagnetic monitoring and urban scale modelling. Atmos. Environ. 92, 130–140.
Zhu, Y., Hinds, W.C., Kim, S., Shen, S., Sioutas, C., 2002. Study of ultrafine particles near a major highway with heavy-duty diesel traffic. Atmos. Environ. 36, 4323–4335.
Iowa Environmental Mesonet, Open Data (https://mesonet.agron.iastate.edu/request/download.phtml?networkTX=_ASOS).
Janssen, N.A.H., Hoek, G., Simic-Lawson, M., Fischer, P., Van Bree, L., Ten Brink, H., Keuken, M., Atkinson, R.W., Anderson, H.R., Brunekreef, B., 2011. Black carbon as an additional indicator of the adverse health effects of airborne particles compared with PM10 and PM2. 5. Environ. Health Perspect. 119 (12), 1691–1699.
Kardel, F., Wuyts, K., Maher, B.A., Samson, R., 2012. Intra-urban spatial variation of magnetic particles: monitoring via leaf saturation isothermal remanent magnetisation (SIRM). Atmos. Environ. 55, 111–120.
Karner, A.A., Eisinger, D.S., Niemeier, D.A., 2010. Near-roadway air quality: synthesizing the findings from real-world data. Environ. Sci. Technol. 44 (14), 5334–5344.
Kaye, J.P., Groffman, P.M., Grimm, N.B., Baker, L.A., Pouyat, R.V., 2006. A distinct urban biogeochemistry? Trends Ecol. Evol. 21 (4), 192–199.
Klink, K., 2015. Seasonal patterns and trends of fastest 2-min winds at coastal stations in the conterminous USA. Int. J. Climatol. 35 (14), 4167–4175.
Lequy, E., Calvaruso, C., Conil, S., Turpault, M.-P., 2014. Atmospheric particulate deposition in temperate deciduous forest ecosystems: interactions with the canopy and nutrient inputs in two beech stands of northeastern France. Sci. Total Environ. 487, 206–215.
Levia, D.F., Michalzik, B., Bischoff, S., Näthe, K., Legates, D.R., Gruselle, M., Richter, S., 2013. Measurement and modeling of diameter distributions of particulate matter in terrestrial solutions. Geophys. Res. Lett. 40 (7), 1317–1321.
Liu, X., Zhang, X., Schnelle-Kreis, J., Jakobi, G., Cao, X., Cyrys, J., Yang, L., Schloter-Hai, B., Abbaszade, G., Orasche, J., 2020. Spatiotemporal characteristics and driving factors of black carbon in augsburg, Germany: combination of mobile monitoring and street view images. Environ. Sci. Technol. 55 (1), 160–168.
Lovett, G.M., Lindberg, S.E., 1984. Dry deposition and canopy exchange in a mixed oak forest as determined by analysis of throughfall. J. Appl. Ecol. 1013–1027.
Luce, B.W., Barrett, T.E., Ponette-González, A.G., 2020. Student cyclists experience PM2. 5 pollution hotspots around an urban university campus. Geogr. Bull. 61 (2).
Maher, B.A., Moore, C., Matzka, J., 2008. Spatial variation in vehicle-derived metal pollution identified by magnetic and elemental analysis of roadside tree leaves. Atmos. Environ. 42 (2), 364–373.
Masson-Delmotte, V., Zhai, P., Pirani, A., Connors, S.L., Péan, C., Berger, S., Caud, N., Chen, Y., Goldfarb, L., Gomis, M.I., 2021. Climate Change 2021: the Physical Science Basis. Contribution of Working Group I to the Sixth Assessment Report of the Intergovernmental Panel on Climate Change. IPCC Geneva, Switz.
Matsuda, K., Sase, H., Murao, N., Fukazawa, T., Khoomsub, K., Chanonmuang, P., Visaratana, T., Khummongkol, P., 2012. Dry and wet deposition of elemental carbon on a tropical forest in Thailand. Atmos. Environ. 54, 282–287.
Mori, J., Fini, A., Galimberti, M., Ginepro, M., Burchi, G., Massa, D., Ferrini, F., 2018. Air pollution deposition on a roadside vegetation barrier in a mediterranean environment: combined effect of evergreen shrub species and planting density. Sci. Total Environ. 643, 725–737.
Petzold, A., Ogren, J.A., Fiebig, M., Laj, P., Li, S.-M., Baltensperger, U., Holzer-Popp, T., Kinne, S., Pappalardo, G., Sugimoto, N., 2013. Recommendations for reporting" black carbon" measurements. Atmos. Chem. Phys. 13 (16), 8365–8379.
Ponette-González, A.G., Ewing, H.A., Weathers, K.C., 2016. Interactions between precipitation and vegetation canopies. In: A Biogeoscience Approach to Ecosystems. Cambridge University Press, New York, pp. 215–253.
Ponette-González, A.G., Van Stan II, J.T., Magyar, D., 2020. Things seen and unseen in throughfall and stemflow. In: Precipitation Partitioning by Vegetation. Springer, pp. 71–88.
Ponette-González, A.G., 2021. Accumulator, transporter, substrate, and reactor: multidimensional perspectives and approaches to the study of bark. Front. Forests Global Change 116.
Popek, R., Haynes, A., Przybysz, A., Robinson, S.A., 2019. How much does weather matter? Effects of rain and wind on PM accumulation by four species of Australian native trees. Atmosphere (Basel) 10 (10), 633.
Przybysz, A., Sæbø, A., Hanslin, H.M., Gawroński, S.W., 2014. Accumulation of particulate matter and trace elements on vegetation as affected by pollution level, rainfall and the passage of time. Sci. Total Environ. 481, 360–369.
Pugh, T.A.M., MacKenzie, A.R., Whyatt, J.D., Hewitt, C.N., 2012. Effectiveness of green infrastructure for improvement of air quality in urban street canyons. Environ. Sci. Technol. 46 (14), 7692–7699.
QGIS, 2021. QGIS Geographic Information System. QGIS Association. http://www.qgis.org.
Rea-Downing, G., Quirk, B.J., Wagner, C.L., Lippert, P.C., 2020. Evergreen needle magnetization as a proxy for particulate matter pollution in urban environments. GeoHealth 4 (9), e2020GH000286.
Rindy, J.E., Ponette-González, A.G., Barrett, T.E., Sheesley, R.J., Weathers, K.C., 2019. Urban trees are sinks for soot: elemental carbon accumulation by two widespread oak species. Environ. Sci. Technol. 53 (17), 10092–10101.
Sohn, G., Dowman, I., 2007. Data fusion of high-resolution satellite imagery and LiDAR data for automatic building extraction. ISPRS J. Photogrammetry Remote Sens. 62 (1), 43–63.
Southerland, V.A., Anenberg, S.C., Harris, M., Apte, J., Hystad, P., van Donkelaar, A., Martin, R.V., Beyers, M., Roy, A., 2021. Assessing the distribution of air pollution health risks within cities: a neighborhood-scale Analysis leveraging high-resolution data sets in the bay area. California. Environ. Health Perspect. 129 (3), 37006.
State of the Denton Urban Forest. 2016 Retrieved from, https://www.itreetools.org/resources/reports/2016_State_of_the_Denton_Urban_Forest_Preservation_Tree.pdf.
Torres, A., Bond, T.C., Lehmann, C.M.B., Subramanian, R., Hadley, O.L., 2014. Measuring organic carbon and black carbon in rainwater: evaluation of methods. Aerosol Sci. Technol. 48 (3), 239–250.
U.S. Census Bureau, 2020. Quick facts. Retrieved from. https://www.census.gov/quickfacts/fact/table/dentoncitytexas/LND110210.
Van Stan II, J.T., Siegert, C.M., Levia Jr., D.F., Scheick, C.E., 2011. Effects of wind-driven rainfall on stemflow generation between codominant tree species with differing crown characteristics. Agric. For. Meteorol. 151 (9), 1277–1286.
Van Stan, J.T., Ponette-González, A.G., Swanson, T., Weathers, K.C., 2021. Throughfall and stemflow are major hydrologic highways for particulate traffic through tree canopies. Front. Ecol. Environ. 19, 404–410.
Vardoulakis, S., Fisher, B.E.A., Pericleous, K., Gonzalez-Flesca, N., 2003. Modelling air quality in street canyons: a review. Atmos. Environ. 37 (2), 155–182.
Wang, L., Gong, H., Peng, N., Zhang, J.Z., 2018. Molecular adsorption mechanism of elemental carbon particles on leaf surface. Environ. Sci. Technol. 52 (9), 5182–5190.
Weather Underground. Wunderground [Online]. https://www.wunderground.com.
Weathers, K.C., Ponette-González, A.G., 2011. Atmospheric deposition. In: Levia, D., Carlyle-Moses, D.E., Tanaka, T. (Eds.), Forest Hydrology and Biogeochemistry: Synthesis of Past Research and Future Directions. Springer Netherlands, pp. 357–370.
Weathers, K.C., Cadenasso, M.L., Pickett, S.T.A., 2001. Forest edges as nutrient and pollutant concentrators: potential synergisms between fragmentation, forest canopies, and the atmosphere. Conserv. Biol. 15 (6), 1506–1514.
Weathers, K.C., Simkin, S.M., Lovett, G.M., Lindberg, S.E., 2006. Empirical modeling of atmospheric deposition in mountainous landscapes. Ecol. Appl. 16 (4), 1590–1607.
Wilson, J.G., Kingham, S., Pearce, J., Sturman, A.P., 2005. A review of intraurban variations in particulate air pollution: implications for epidemiological research. Atmos. Environ. 39 (34), 6444–6462.
Xie, M., Coons, T.L., Dutton, S.J., Milford, J.B., Miller, S.L., Peel, J.L., Vedal, S., Hannigan, M.P., 2012. Intra-urban spatial variability of PM2.5-bound carbonaceous components. Atmos. Environ. 60, 486–494.
Xie, C., Kan, L., Guo, J., Jin, S., Li, Z., Chen, D., Li, X., Che, S., 2018. A dynamic processes study of PM retention by trees under different wind conditions. Environ. Pollut. 233, 315–322.
Xu, X., Zhang, Z., Bao, L., Mo, L., Yu, X., Fan, D., Lun, X., 2017. Influence of rainfall duration and intensity on particulate matter removal from plant leaves. Sci. Total Environ. 609, 11–16.
Xu, X., Xia, J., Gao, Y., Zheng, W., 2020. Additional focus on particulate matter wash-off events from leaves is required: a review of studies of urban plants used to reduce airborne particulate matter pollution. Urban For. Urban Green. 48, 126559.
Xu, H., Ren, Y., Zhang, W., Meng, W., Yun, X., Yu, X., Li, J., Zhang, Y., Shen, G., Ma, J., 2021. Updated global black carbon emissions from 1960 to 2017: improvements, trends, and drivers. Environ. Sci. Technol. 55 (12), 7869–7879.
Zhang, L., Zhang, Z., Chen, L., McNulty, S., 2019. An investigation on the leaf accumulation- removal efficiency of atmospheric particulate matter for five urban plant species under different rainfall regimes. Atmos. Environ. 208, 123–132.